

Alkanethiol Mediated Release of Surface Bound Nanoparticles Fabricated by Nanosphere Lithography

Jing Zhao, Amanda J. Haes, * Xiaoyu Zhang, Shengli Zou, Erin M. Hicks, George C. Schatz, and Richard P. Van Duyne

Northwestern University, Department of Chemistry, 2145 Sheridan Road, Evanston, Illinois 60208-3113

*Current address: Naval Research Laboratory, Washington D.C.

ABSTRACT

This work presents an innovative approach to produce monodisperse solution-phase triangular silver nanoparticles with well-controlled geometry. Ag nanotriangles are fabricated by nanosphere lithography (NSL), functionalized with alkanethiol molecules and then released from the substrate into solution. The resulting single isolated nanoparticles are subsequently asymmetrically functionalized with alkanedithiol molecules to form dimer pairs. The optical properties of the Ag nanoparticles have been measured using UV-Vis spectroscopy while their structural properties have been characterized using atomic force microscopy (AFM) and transmission electron microscopy (TEM). Theoretical calculations based on Mie theory and the Discrete Dipole Approximation (DDA) method have been done to interpret the optical properties of the released Ag nanoparticles.

INTRODUCTION

There is currently a great interest in studying the optical properties of metal particles in the nanoscale. Metal nanoparticles have distinctive optical properties that are not available in either isolated molecules or bulk solids. The most important optical excitation in noble metal nanoparticles is localized surface plasmon resonances (LSPR).¹⁻³ When metal nanoparticles are excited by electromagnetic radiation, they exhibit collective oscillations of their conduction electrons known as localized surface plasmons. Recent investigations have revealed that the optical properties of the nanoparticles highly depend on their geometry, metal composition, and the surrounding dielectric environment.^{4,5}

Traditionally, noble metal nanoparticles are produced by the reduction of a metal salt in solution. Alternative fabrication methods based on electron beam lithography (EBL),⁶ focused ion beam lithography (FIB),⁷ and nanosphere lithography (NSL)⁸⁻¹⁰ have been developed to fabricate nanoparticles confined on solid substrates. NSL inexpensively produces nanoparticle arrays with precisely controlled geometry and interparticle spacing. By changing the size of the nanospheres, deposited material and metal thickness, NSL has been developed to fabricate nanoparticles with tunable LSPR wavelengths (λ_{\max}).^{1,11}

The optical properties of metal nanoparticles can be modeled by the classical

electromagnetic approaches. Mie theory¹² is widely used to simulate the scattering of light by a spherical particle. A numerical method, discrete dipole approximation (DDA) method, has been used to model the optical properties of object with arbitrary shapes in various dielectric environments. In the DDA method, the particle of interest is represented by a polarizable cubic array. The induced dipole polarizations in these cubes are determined self-consistently, and then properties such as the extinction cross section are determined in terms of the induced polarizations.¹³

It has been reported previously that the NSL fabricated Ag nanoparticle adhesion to glass is not strong; that is, less than 10 nN (normal force) is required to remove the Ag nanoparticles from glass.¹⁴ Based on this property, we have developed a method to intentionally remove the NSL fabricated Ag nanoparticles from the glass substrate and produce size-controlled monodisperse Ag nanoparticles in solution. To stabilize the nanoparticles in solution, the nanoparticles are functionalized with alkanethiol molecules before their release. Notice that the bottom sides of these nanoparticles are not functionalized during the stabilization process, alkanedithiol molecules are used to asymmetrically link the released nanoparticles in solution.¹⁵ The dramatic spectral change induced by the release and linking of the nanoparticles has been monitored with UV-Vis spectroscopy experimentally, and simulated with Mie theory and the DDA method.

EXPERIMENTAL SECTION

Nanoparticle Fabrication and Functionalization

NSL was used to create surface-confined Ag nanotriangles.⁸ Polystyrene nanospheres with diameter = 400 nm were used to create the template and 50 nm silver was deposited through the template. A schematic illustration of the functionalization process is displayed in Figure 1. Immediately after the removal of the nanosphere mask, the samples were placed in 1 mM hexadecanethiol (in ethanol) for 48-96 hours. A well-order self-assembled monolayer (SAM) of hexadecanethiol formed over the nanoparticles during incubation. The samples were then

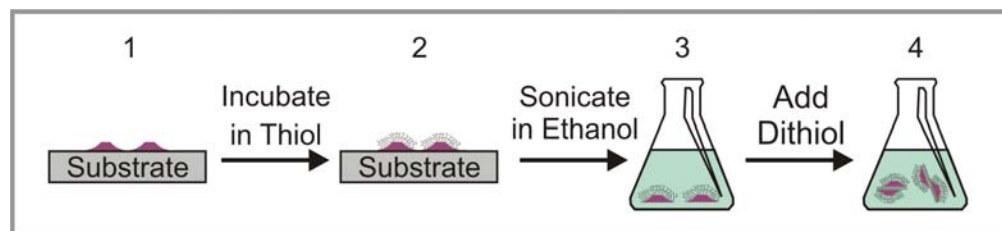


Figure 1 The fabrication and functionalization of solution-phase Ag nanoparticles in four steps. (1) Fabrication of Ag nanoparticles on a glass substrate by NSL. (2) Incubation in 1 mM 1-hexadecanethiol solution to form a SAM of 1-hexadecanethiol. (3) Sonication in ethanol to release the Ag nanoparticles in solution. And (4) addition of 1,6-hexanedithiol molecules to linked two Ag nanoparticles asymmetrically.

thoroughly rinsed with ethanol, and sonicated in neat ethanol for ~3 min to release the SAM-coated nanoparticles into solution. The nanoparticle solution was filtered with 400 nm filters (GE Osmonics, Inc. Minnetonka, MN) to remove large particles arising from defects in the nanosphere mask. To asymmetrically link the nanoparticles, ~2 μL of 1 mM 1,6-hexanedithiol ethanol solution was added during the releasing sonication process.

Atomic Force Microscopy and Transmission Electron Microscopy

Atomic force microscope (AFM) images were collected using a Digital Instruments Nanoscope IV microscope and Nanoscope IIIa controller operating in tapping mode.

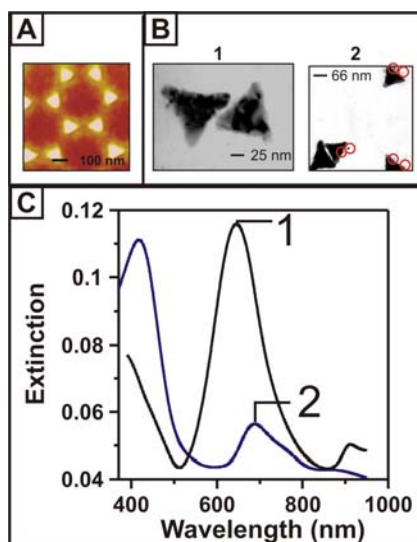


Figure 2 Morphology and extinction spectra of Ag nanoparticles coated with a SAM of 1-hexadecanethiol molecules. (A) AFM image of NSL fabricated Ag nanoparticles on a glass substrate. (B) TEM images of solution-phase Ag nanoparticles. Image 2B-1 shows two representative triangular Ag nanoparticles. Image 2B-2 reveals the existence of some small spherical nanoparticles (red circle) which are the fragments of the triangular particles arising from sonication. (C) Extinction spectra of Ag nanoparticles confined on a glass substrate (spectrum 2C-1) and released in ethanol solution (spectrum 2C-2). All the extinction measurements are performed in ethanol environment.

Transmission electron microscope (TEM) images were collected using a Hitachi 8100 TEM.

Ultraviolet-Visible Extinction Spectroscopy

The extinction maximum, λ_{max} , of each sample was monitored and recorded using a UV-Vis spectrometer. Macroscale UV-Vis extinction measurements were collected using an Ocean Optics (Dunedin, FL) SD2000 fiber optically coupled spectrometer with a CCD detector. All spectra in this study are performed in standard transmission geometry with unpolarized light. Solution-phase measurements were collected in quartz cuvettes (pathlength = 1 cm).

RESULTS AND DISCUSSION

Optical and Structural Characterizations

Surface-bound triangular Ag nanoparticles are fabricated using NSL and functionalized with alkanethiol SAM with different number of methylene groups. These alkanethiol molecules have similar abilities to stabilize the nanoparticles. Representative data from a 1-hexadecanethiol SAM are presented below.

Figure 2A shows an AFM image of the SAM-coated nanoparticles. AFM reveals nanoparticles with an average height of 52 nm and perpendicular bisectors of ~100 nm. The corresponding extinction spectrum is collected in ethanol and displayed in Figure 2C-1. The extinction maximum is at 638 nm.

Following SAM functionalization, the Ag nanoparticles have been well-rinsed and released into solution by sonication in ethanol. A dramatic change in the UV-Vis extinction spectrum is observed. Two peaks appear in the spectrum--an intense peak appears at 418 nm and a weak broad peak centered at 682 nm. Since the structure of the nanoparticles has a significant effect on their optical properties, TEM is used to reveal the morphology of the solution-phase nanoparticles. The TEM images of the released nanoparticles are displayed in Figure 2B. Figure 2B-1 demonstrates that the solution-phase nanoparticles have a perpendicular bisector of ~ 100 nm, which is in good agreement with AFM measurement. Furthermore, the curved triangular edges of the nanoparticles coming from the footprints of the nanospheres template have been clearly seen with TEM. Upon a closer examination of a larger scale TEM image of the solution-phase nanoparticle, as displayed in Figure 2B-2 (red circles), many small spherical

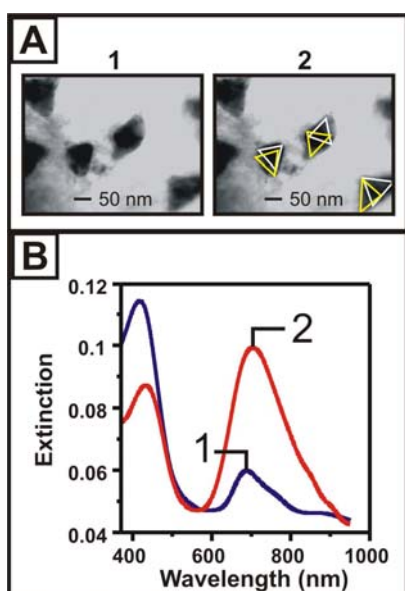


Figure 3 Morphology and extinction spectra of solution-phase Ag nanoparticles. (A) TEM 3A-1 reveals asymmetrically linked Ag nanoparticles dimers with various degrees of overlap. TEM 3A-2 is the same image as image 1 with triangular frames guiding for the recognition of dimer formation. (B) Extinction spectra of Ag nanoparticle monomers (spectrum 3B-1) and dimers (spectrum 3B-2) in ethanol solution.

nanoparticles are observed over the nanoparticle solution samples. The origin of these small spherical nanoparticles is still under investigation. However, we have proposed two possibilities. First, the sphere packing defect in NSL may result in smaller particles after metal deposition.¹ Second, we posit that sonication may disrupt and fracture some of the NSL fabricated nanotriangles into smaller nanoparticles.

During the releasing process described above, all sides of the released nanoparticles are coated with SAM of 1-hexadecanethiol except for their bases. 2 μL of 1 mM 1,6-hexanedithiol ethanol solution was added to the nanoparticle solution to functionalize the bases and then asymmetrically link the nanoparticles. The formation and geometry of nanoparticle dimers are proved by TEM (image shown in Figure 3A-1). Upon overlaying triangular frames onto the TEM image (Figure 3A-2), it appears that slightly mismatched nanoparticle dimers formed. The resulting dimers have perpendicular bisectors ranging from ~ 90 nm to 165 nm. During the formation of nanoparticle dimers, an immediate change in the UV-Vis spectrum of the nanoparticle solution is observed and shown in Figure 3B, Spectrum 2. Compared with the UV-Vis spectrum of the nanoparticle monomer solution (3B-1), the extinction maximum located at 418 nm (3B-1) shifts to 431 nm (3B-2) and decreases in intensity while the local maximum located at 682 nm (3B-1) shifts to 705 nm (3B-2) and increases in intensity and peak width.

Theoretical Calculations

As revealed in the TEM images in Figure 2B, there are two major types of Ag nanoparticles in the released nanoparticle monomer solution: (1) small spherical fragments and (2) truncated tetrahedral Ag nanoparticles. Mie theory has been used to model 1-hexadecanethiol SAM-coated spherical Ag nanoparticles with radii ranging from 5, 10, 15, to 20 nm. Figure 4A shows that as the sphere radius increases, the LSPR extinction maximum increases from 390 nm to 410 nm. DDA method has been utilized to model the truncated tetrahedral Ag nanoparticles. Figure 4B presents the in-plane (Figure 4B-1) and out-of-plane (Figure 4B-2) polarized spectra of a single Ag truncated tetrahedron with a hexadecanethiol monolayer. In comparison to the experimental results (Figure 3B), the calculated in-plane polarized spectrum (Figure 4B-1) with the resonance peak located at ~ 710 nm corresponds to the red peak in Figure 3B-1. While the out-of-plane polarization peak (4B-2) located at ~ 500 nm, which combined with the Mie theory modeling of the small spherical nanoparticles, corresponds to the blue experimental maximum. The discrepancy between experimental and calculated spectra arises from the fact that the nanotriangles produced by NSL have slightly rounded tips due to the instinct nature of NSL;⁵ while the geometry of the nanoparticle in the theoretical model has sharp tips.

It has been demonstrated in the TEM image in Figure 3A that the nanoparticle monomers have been asymmetrically linked upon the addition of alkanedithiol. The resulting dimers have different degrees of overlap between two particles. The DDA method is employed to explain the spectral change caused by the formation of dimers. As shown in Figure 4C, the in-plane polarization extinction spectra have been calculated for dimers with various overlap between the two nanoparticles. The calculated extinction maxima are in the range of 725 ± 30 nm for distances d (see inset to Figure. 4C) ranging from 15 nm to 25 nm. This is in good agreement

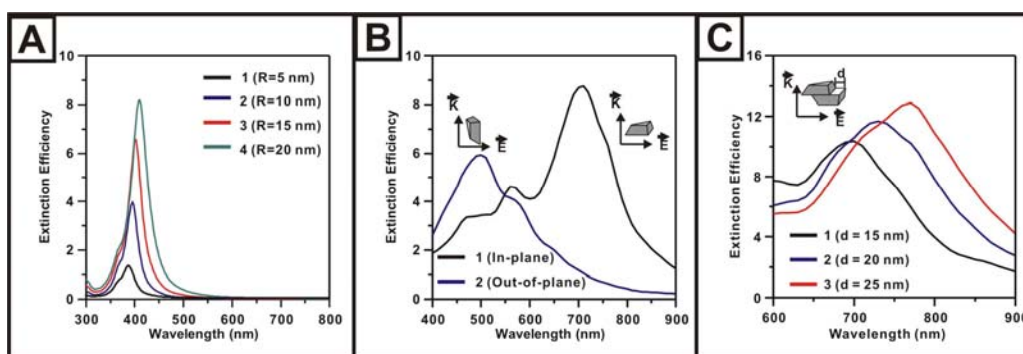


Figure 4 Calculations of the extinction spectra of spherical and triangular Ag nanoparticles coated with a SAM of 1-hexadecanethiol molecules (refractive index $n = 1.45$) in an ethanol environment ($n = 1.36$). (A) Mie theory calculations of the extinction spectra of Ag nanospheres with radii of 5, 10, 15, and 20 nm, respectively. (B) DDA calculations of the extinction spectra of triangular Ag nanoparticles: in-plane polarization (4B-1) and out-of-plane polarization (4B-2). (C) DDA calculations of extinction spectra of a pair of linked Ag nanoparticles. The degree of nonoverlap d between the two bases of the Ag nanotriangles is 15, 20, and 25 nm, respectively.

with the experimental extinction maximum of the nanoparticle dimers located at 705 nm in Figure 3B-2. The overall calculated peaks have a broad peak width, which corresponds to the broadness of the observed peak.

CONCLUSIONS

In this work, we have demonstrated that a novel technique based on the NSL method to fabricate solution-phase triangular nanoparticles with a tunable and well-controlled geometry. 1-hexanedecanethiol molecules have been used to stabilize and to prevent the nanoparticles from aggregation in solution. This technique allows for the asymmetrical functionalization of the nanoparticles when a linking agent (alkanedithiol) is used. Because the geometry of these nanoparticles can be precisely controlled by NSL, they are potentially good candidates for single nanoparticle chemical and biological sensing events.

ACKNOWLEDGMENTS

The authors gratefully acknowledge support from the National Science Foundation (EEC-0118025, CHE-0414554, BES-0507036) and the Air Force Office of Scientific Research MURI program (Grant F49620-02-1-0381).

REFERENCES

1. C. L. Haynes and R. P. Van Duyne, *J. Phys. Chem. B* **105**, 5599 (2001)
2. U. Kreibig, M. Gartz and A. Hilger, *Ber. Bunsen-Ges.* **101**, 1593 (1997)
3. M. A. El-Sayed, *Acc. Chem. Res.* **34**, 257 (2001)
4. T. R. Jensen, K. L. Kelly, A. Lazarides and G. C. Schatz, *Journal of Cluster Science* **10**, 295 (1999)
5. X. Y. Zhang, E. M. Hicks, J. Zhao, G. C. Schatz and R. P. Van Duyne, *Nano Lett* **5**, 1503 (2005)
6. C. L. Haynes, A. D. McFarland, L. L. Zhao, R. P. Van Duyne, G. C. Schatz, L. Gunnarsson, J. Prikulis, B. Kasemo and M. Kall, *J. Phys. Chem. B* **107**, 7337 (2003)
7. M. T. Marshall, M. L. McDonald, X. Tong, M. Yeadon and J. M. Gibson, *Rev Sci Instrum* **69**, 440 (1998)
8. J. C. Hulteen and R. P. Van Duyne, *J. Vac. Sci. Technol. A* **13**, 1553 (1995)
9. U. C. Fischer and H. P. Zingsheim, *J Vac Sci Technol* **19**, 881 (1981)
10. H. W. Deckman and J. H. Dunsmuir, *Appl Phys Lett* **41**, 377 (1982)
11. T. R. Jensen, M. D. Malinsky, C. L. Haynes and R. P. Van Duyne, *J. Phys. Chem. B* **104**, 10549 (2000)
12. G. Mie, *Annalen der Physik (Weinheim, Germany)* **25**, 377 (1908)
13. B. T. Draine and P. J. Flatau, *J. Op. Soc. Am. A* **11**, 1491 (1994)
14. J. C. Riboh, A. J. Haes, A. D. McFarland, C. R. Yonzon and R. P. Van Duyne, *J. Phys. Chem. B* **107**, 1772 (2003)
15. A. J. Haes, J. Zhao, S. L. Zou, C. S. Own, L. D. Marks, G. C. Schatz and R. P. Van Duyne, *J. Phys. Chem. B* **109**, 11158 (2005)